

# A Computational Analysis of Gas Jet Flow Effects on Liquid Aspiration in the Collison Nebulizer

James Q. Feng

**Abstract**—Pneumatic nebulizers (as variations based on the Collison nebulizer) have been widely used for producing fine aerosol droplets from a liquid material. The basic working principle of those nebulizers has been qualitatively described as utilization of the negative pressure associated with an expanding gas jet to syphon liquid into the jet stream, then to blow and shear into liquid sheets, filaments, and eventually droplets. Detailed quantitative analysis based on fluid mechanics theory is desirable, to gain in-depth understanding of the liquid aspiration mechanism among other aspects of the Collison nebulizer behavior. The purpose of present work is to investigate the nature of negative pressure distribution associated with compressible gas jet flow in the Collison nebulizer by a computational fluid dynamics (CFD) analysis, using an OpenFOAM® compressible flow solver. The value of the negative pressure associated with a gas jet flow is examined by varying geometric parameters of the jet expansion channel adjacent to the outlet of jet orifice. Such an analysis can provide valuable insights into fundamental mechanisms in liquid aspiration process, helpful for effective design of improved pneumatic atomizer in the Aerosol Jet® direct-write system for micro-feature, high-aspect-ratio material deposition in additive manufacturing.

**Keywords**—Collison nebulizer, compressible gas jet flow, liquid aspiration, pneumatic atomization.

## I. INTRODUCTION

THE original motivation to develop pneumatic nebulizers was for producing medical aerosols in the inhalation therapy [1]. Among many variations, the Collison nebulizer (introduced by W. E. Collison) has been the most representative one, widely used in applications extended even beyond therapeutic inhalers. For example, the Aerosol Jet® direct-write systems typically include a pneumatic atomizer with similar configuration as the Collison nebulizer, for producing aerosol droplets of functional ink material in the size range of 1–5  $\mu\text{m}$  [2, 3]. This type of pneumatic nebulizer has shown capabilities of effectively atomizing liquid materials much more viscous than the usual therapeutic liquids, enabling Aerosol Jet® to print inks with high concentrations of functional materials. To further improve the pneumatic atomizer performance in Aerosol Jet® systems, it is important to understand detailed fluid dynamics and the effects of various parameters involved in the atomizer design.

Despite its wide usage in a variety of applications, the technical details about fluid dynamic behavior of the Collison nebulizer can rarely be found in the current literature. The only noticeable paper is that published by May in 1973 [1], providing some design details and various experimental data through scientific measurements. Although there were a few

later publications [4, 5] offering more data regarding some functional aspects of various pneumatic, or air-jet, nebulizers, the discussion of basic working principle remained at the level of qualitative hand-waving.

Here in this work, a computational fluid dynamics (CFD) analysis is conducted to investigate effects of atomizer geometric parameters on the compressible gas jet flow behavior based on a Collison nebulizer configuration. The results can provide valuable insights into the process of liquid aspiration, as a key player in the Collison nebulizer functionality, which can lead to effective design of improved pneumatic atomizers for the Aerosol Jet® systems.

## II. PROBLEM DESCRIPTION

### A. Working Principle of the Collison Nebulizer

As described by May [1], the Collison nebulizer (schematically shown in Fig. 1) consists of a small jet orifice that produces a jet around sonic speed as compressed gas flows through it. Such a jet formed from compressed gas would expand in the jet expansion channel downstream of the jet orifice, creating a reduction of local static pressure (or “negative pressure”) to suck liquid ink through the ink syphon tube. Thus, the ink syphoned into the jet stream region can then form liquid sheets, filaments, and droplets under the strong shear of high-speed jet flow. No active liquid pump is used here, remarkably.

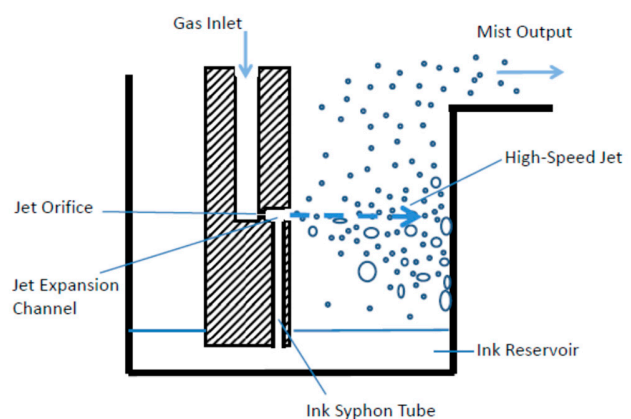


Fig. 1 Schematic of a typical configuration of the Collison nebulizer

However, the liquid droplets produced by such a blowing gas jet often have a very wide size distribution. To remove droplets larger than 5  $\mu\text{m}$  or so, the droplets carried by the jet flow are directed toward the wall of nebulizer chamber, where large droplets with sufficient mass are blown onto by inertial impaction. Only a small fraction (typically < 0.1%) of the liquid syphoned into jet stream can become fine enough

J. Q. Feng is with Optomec, Inc., St. Paul, MN 55114 USA (corresponding author, phone: 1-651-200-6508; e-mail: jfeng@optomec.com).

droplets (e.g.,  $< 5 \mu\text{m}$ ) to escape impact and be carried by the gas flow as the output mist [1].

Because more than 99.9% of the liquid ink going through the atomization process might be cycled back to the ink reservoir, the liquid aspiration rate through the ink syphon tube is expected to substantially influence the output mist density of the nebulizer. Sufficient liquid aspiration rate requires sufficient negative pressure in the jet expansion channel. For a given aspiration rate, an ink with higher viscosity needs stronger negative pressure. Thus, the magnitude of negative pressure generated in the jet expansion channel by compressible gas jet flow becomes the subject of study in this paper.

### B. Atomization Behavior of the Collision Nebulizer

Many applications desire high liquid mass output from the nebulizer, which is probably why the Collision nebulizer typically operates with a gas flow rate  $Q > 2000$  sccm (per jet), through a jet orifice typically of diameter  $D = 0.35$  mm. It has commonly observed that the liquid mass density in output mist (also known as the mist density) decreases with the gas flow rate, although the liquid mass output still increases for  $Q > 2000$  sccm [1]. This fact suggests that beyond 2000 sccm the increase of liquid atomization rate cannot catch up the increase of gas flow rate.

In contrast, for Aerosol Jet® direct-write applications, the output mist density generated from its (Collision-type) pneumatic atomizer is much more relevant to the desired high printing throughput. Depending on ink materials, it has been found more often than not that the peak mist density is obtained at a gas flow rate around  $Q = 1200$  sccm; further increasing the gas flow rate rather yields lower mist density. With more careful experimentations, most inks for Aerosol Jet® printing are found to yield mist output at a gas flow rate greater than  $Q = 600$  sccm.

In the standard Collision nebulizer configuration, the atomization jet (as well as the jet expansion channel) is located about  $h = 20$  mm above the liquid level in the ink reservoir (cf. Fig. 1). To bring ink through its syphon tube from the reservoir up to the jet stream for atomization, the pressure in jet expansion channel must be reduced to a level at least enough to overcome the hydrostatic pressure  $\rho_{\text{ink}} g h$  with  $\rho_{\text{ink}}$  denoting the ink density and  $g (= 9.81 \text{ m s}^{-2})$  the gravitational acceleration. Most metal nanoparticle inks for Aerosol Jet® in printing electronic devices often have  $\rho_{\text{ink}}$  about 2 g/cc. Thus the hydrostatic pressure  $\rho_{\text{ink}} g h$  may be estimated as about 400 Pa. In other words, the reduction of pressure (also known as the “negative pressure”) in jet expansion channel from the atomizer chamber pressure (which is usually very close to the ambient value, e.g.,  $10^5$  Pa) must be greater than 400 Pa (plus or minus about 100 Pa due to the capillary effect depending on the contact angle and surface tension of the ink) at a gas flow rate of  $Q = 600$  sccm.

When the volumetric flow rate  $Q$  of compressible gas flow is measured in units of “standard cubic centimeters per minute” (sccm), the actual volumetric flow rate varies with temperature but the mass flow rate remains as a constant.

Thus, the value of  $\rho U = 4 \rho_s Q / (\pi D^2)$  is a constant for given  $Q$  and  $D$ , with  $\rho$  and  $\rho_s$  denoting the actual density of gas and that under standard conditions at  $T_s = 273$  K and  $P_s = 10^5$  Pa, e.g.,  $\rho_s = P_s / (R T_s) = 1.276 \text{ kg/m}^3$  for dry air (which is about the same as the dry nitrogen typically used as the inert carrier gas in Aerosol Jet® systems). The value of the jet Reynolds number  $Re = \rho U D / \mu$  can be calculated as  $1.464 Q / D$  with  $Q$  in units of sccm and  $D$  in millimeters assuming the dynamic viscosity of gas  $\mu = 1.85 \times 10^{-5} \text{ kg m}^{-1} \text{ s}^{-1}$  (at  $T = 300$  K). Hence  $Re = 5018$  with  $Q = 1200$  sccm and  $D = 0.35$  mm, while  $Re = 2509$  for  $Q = 600$  sccm.

### C. The CFD Model

The mathematical model considered here is for fluid dynamics simulation of a compressible gas flowing from an inlet channel through a small jet orifice into a jet expansion channel of larger diameter and then into a much large atomization chamber with a solid wall at its end. For simplicity without loss of the essence of the problem, all the involved channels are arranged concentrically such that the computational domain becomes axisymmetric (with negligible effect of gravity in such a microscale gas flow).

As a nominal model setting, the jet orifice has a diameter of  $D = 0.35$  mm and the diameter and length of jet expansion channel are  $D_e = 1.5$  mm and  $L_e = 2.7$  mm, to be consistent with the standard Collision nebulizer design [1]. To complete model construction, the computational domain also contains an entrance tube of 3 mm diameter upstream of the jet orifice and a large cylindrical chamber with diameter of 7 mm and length of 14 mm downstream of the jet expansion channel (as shown in Fig. 2).

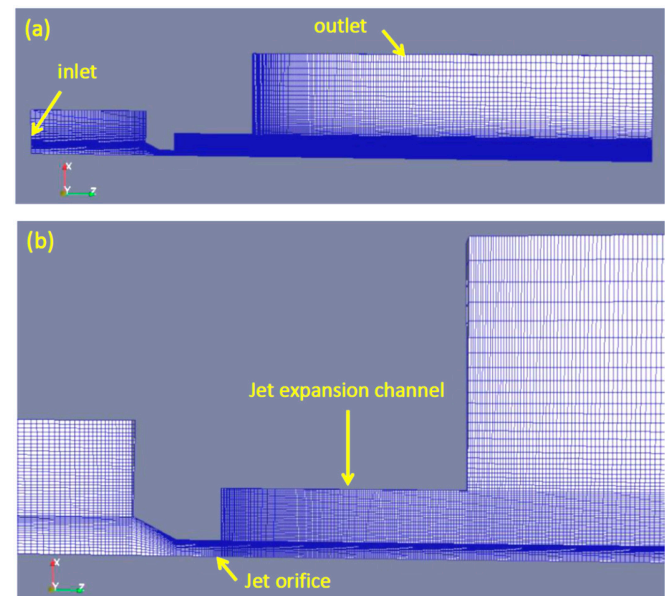


Fig. 2 (a) Complete, and (b) regional details of the computational domain with a wedge type mesh for axisymmetric problem, generated with the *blockMesh* utility

Except the axis of symmetry, the inlet patch at the upstream end of the entrance tube and the outlet patch as the cylindrical

side of the large atomization chamber, all other physical boundaries of the computational domain are treated as solid walls.

Among several choices, the steady compressible flow solver known as *rhoSimpleFoam*, available in the OpenFOAM® CFD Toolbox v.2.4.0 [6], is used for computing solutions of the Navier-Stokes equation system (which includes equations for conservations of mass, momentum, and energy, governing the flow of a fluid described by the ideal gas law and Fourier's law of heat conduction with Sutherland's law for dynamic viscosity). This solver also contains a variety of turbulence models. The 3D meshing utility *blockMesh*, included in the OpenFOAM® package, is used to generate mesh according to the computational domain (in Fig. 2).

The boundary conditions for flow velocity  $U$ , pressure  $p$ , and temperature  $T$  at solid walls are *fixedValue* (for  $U = 0$ ), *zeroGradient* (for  $p$ ), and *fixedValue* ( $T = 300\text{K}$ ), at inlet *flowRateInletVelocity* (for  $U$  with a specified mass flow rate), *zeroGradient* (for  $p$ ), and *fixedValue* ( $T = 300\text{K}$ ), and at outlet *pressureInletOutletVelocity* (for  $U$ ), *fixedValue* (for  $p = 10^5$  Pa), and *zeroGradient* (for  $T$ ), respectively.

Based on estimated values of the jet Reynolds number (e.g.,  $\sim 2500$  at  $Q = 600$  sccm, etc.), the free jet flow out of the small orifice (with  $D = 0.35$  mm) is expected to be turbulent [7, 8]. Thus some kind of turbulence model should be included in the present CFD model. For lack of better knowledge, a common  $k-\epsilon$  model is used here based on Reynolds Averaged Navier-Stokes (RANS) equations, which is (among others) available in the *rhoSimpleFoam* solver.

### III. RESULTS

It is usually difficult to obtain converged solutions by running the *rhoSimpleFoam* solver from a simple default initial condition. In the present work, the corresponding transient flow solver known as *rhoPimpleFoam*, also available in OpenFOAM®, is used for computing compressible flow solutions over certain time span to supply more reasonable initial conditions for the *rhoSimpleFoam* solver to compute the steady-state solutions.

#### A. The Nominal Case

For the nominal case with jet orifice of  $D = 0.35$  mm with a jet expansion channel of  $D_e = 1.5$  mm and  $L_e = 2.7$  mm, the computed results of gas flow field in terms velocity magnitude  $|U|$  and pressure  $p$  with a gas flow rate of  $Q = 1200$  sccm are shown in Fig. 3. At the exit of the jet orifice, the jet velocity can approach 246 m/s, corresponding to a Mach number  $Ma = 0.746$ . Then, the jet expands with velocity decreasing as it moves forward. A significant region of negative pressure  $\Delta P \sim 1524$  Pa indeed appears in the jet expansion channel, providing the syphoning effect for liquid aspiration. Somehow the pressure field does not exhibit similar distribution structure as that of the flow velocity. The lowest pressure zone does not coincide with that of highest velocity as anticipated from Bernoulli's principle.

The computed results of gas density  $\rho$  and temperature  $T$  at  $Q = 1200$  sccm are shown in Fig. 4. The peak value of gas

density ( $\rho = 1.65$  kg/m<sup>3</sup>) upstream to the jet orifice matches that calculated for  $p = 1.425 \times 10^5$  Pa and  $T = 300$  K according to the ideal gas law for dry air (i.e., 1.655 kg/m<sup>3</sup>). The value minimum  $T$  ( $= 270$  K) matches that calculated according to the standard 1D isentropic flow theory [9], i.e.,  $T = 300/(1 + 0.2 Ma^2)$ , (with a specific heat ratio of 1.4 and  $Ma = 0.746$ , which yields 269.95 K). Both the  $\rho$  field and  $T$  field in Fig. 4 display similar structures as that of the  $|U|$  field in Fig. 3, with slightly higher density and lower temperature in the high-speed jet velocity region.

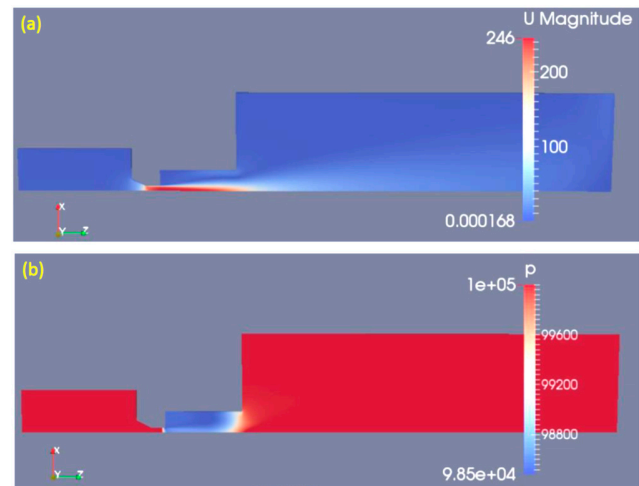


Fig. 3 (a) The field of gas flow velocity magnitude  $|U|$  (m/s) and (b) pressure  $p$  (Pa) for the nominal case configuration at  $Q = 1200$  sccm

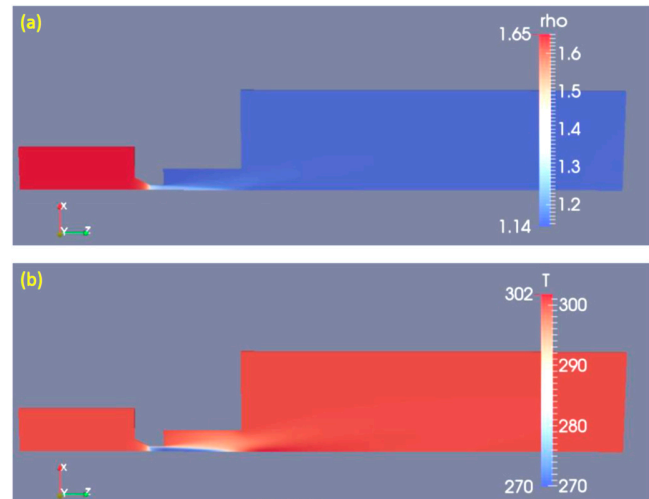


Fig. 4 (a) The field of gas density  $\rho$  (kg/m<sup>3</sup>), and (b) gas temperature  $T$  (K) for the nominal case configuration at  $Q = 1200$  sccm

The profiles of axial velocity component  $U_z$  are plotted in Fig. 5 as functions of radial distance  $r$  (in units of mm), labeled according to the axial distance  $z$  (in units of mm) from the exit of jet orifice. At  $z = 0.5$  mm (close to the jet orifice), the  $U_z$  profile looks quite similar to that of an incompressible gas jet at the nozzle exit [10], having nearly a plug flow profile with very high shear along the jet edge. As the jet



moves away from the orifice, the curves of  $U_z$  at  $z = 1.5$  and  $2.5$  mm show that the edge of the plug flow profile diffuses out while the jet velocity declines with the axial distance. For  $z < 2.7$  mm (within the jet expansion channel), there is a back flow region (as indicated by negative  $U_z$ ) near the channel wall surrounding the jet as a consequence of mass conservation. The back flow disappears as the free jet moves outside the jet expansion channel into the atomization chamber, where the jet stream widens with further reduced velocity due to viscous diffusion (as seen in experiments [7]).

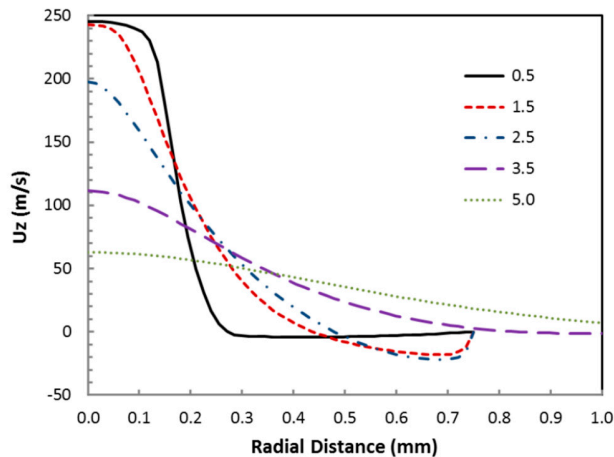


Fig. 5 Radial profiles of axial velocity component  $U_z$  in the nominal configuration for  $Q = 1200$  sccm at axial distance  $z = 0.5, 1.5, 2.5, 3.5, 5.0$  mm from the exit of jet orifice

Corresponding to Fig. 5, the radial profiles of pressure (in units of bar) are plotted in Fig. 6. A generally positive pressure gradient in the axial direction is consistent with declining jet velocity with  $z$ , and the back flow in the jet expansion channel shown in Fig. 5. Each curve shows that the gas pressure generally decreases from jet center with radial distance at a given axial distance  $z$ , with a minimum located close to the channel wall where the back flow magnitude is considerably large. So, the lowest pressure does not appear in the region of highest gas velocity at the jet center, according to an intuitive imagination based on Bernoulli's principle. From the fluid dynamics point of view, an expanding gas jet flow is expected to relate to a decreasing pressure in the radial direction; a decreasing jet velocity with axial distance  $z$  should correspond to a positive pressure gradient with respect to  $z$ , i.e.,  $dp/dz > 0$ . Due to viscous drag, the jet flow tends to bring more gas out of the jet expansion channel than what is supplied from the exit of jet orifice, which creates a reduced local pressure to drive the back flow for compensating the jet depleted gas. Thus, a region of negative pressure appears in the jet expansion channel.

Even out of the jet expansion channel at  $z = 3.5$  and  $5.0$  mm, a negative pressure about 20 Pa appears near the radial distance  $r = 0.75$  mm and about 5 Pa near  $r = 1.2$  mm, respectively. Such a negative pressure around the jet was sometimes used to suck smoke generated by a nearby smoke wire for the jet flow visualization experiments [8]. Near the jet

center, the pressure is higher at  $z = 3.5$  mm with higher gas velocity than that at  $z = 5.0$  mm, while the central pressure generally exhibits lower value with higher jet speed inside the jet expansion channel.

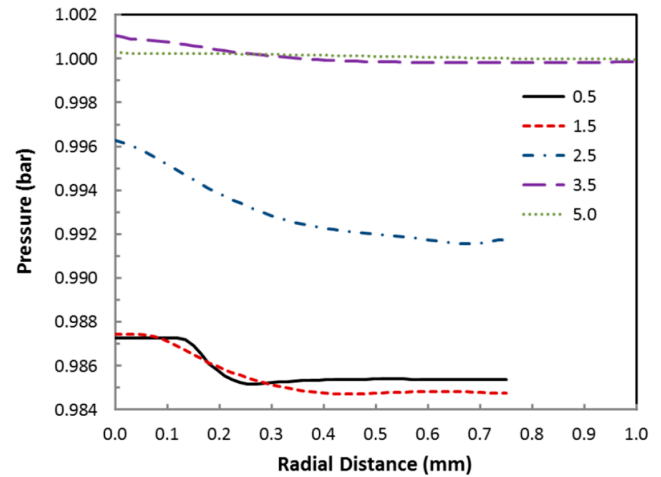


Fig. 6 As Fig. 5 but for radial profiles of pressure  $p$  (in units of bar)

Table I shows the CFD results for maximum jet velocity  $U_{\max}$  and its corresponding Mach number  $Ma_{\max}$ , the value of negative pressure  $\Delta P$  (defined as the pressure value at the wall of jet expansion channel 1.5 mm from the exit of jet orifice subtracted from the atomization chamber pressure  $10^5$  Pa = 1 bar), the gauge pressure upstream to the jet orifice  $P_g$  ( $= p_{\max} - 1.0$  bar where 1 bar =  $10^5$  Pa), and minimum gas temperature in the jet flow  $T_{\min}$ , at various gas flow rates.

TABLE I  
COMPUTED VALUES FOR THE NOMINAL CASE

$Q$ (sccm)	$U_{\max}$ (m/s)	$Ma_{\max}$	$\Delta P$ (Pa)	$P_g$ (bar)	$T_{\min}$ (K)
600	136	0.397	378	0.111	291
900	194	0.576	862	0.241	281
1200	246	0.746	1524	0.425	270
1500	291	0.903	2218	0.662	258
1800	329	1.046	2755	0.927	246

Interestingly, with a gas flow rate of  $Q = 600$  sccm the present CFD model indeed predicts a negative pressure of  $\Delta P \sim 380$  Pa in most part of the jet expansion channel, consistent with expected minimum values estimated based on hydrostatic pressure and capillary effect as well as empirical knowledge. Also consistent with the theoretical expectation as well as measurements of various pneumatic atomizers [1][4], the value of 'air pressure'  $P_g$  increases monotonically with the gas flow rate  $Q$  though the correlation is not exactly linear.

The magnitude of negative pressure obviously increases with the jet velocity and Mach number  $Ma$ . For a jet flow with  $Ma < 1$ , the structure of subsonic gas flow field remains more or less the same as that shown in Fig. 3 and Fig. 4. When the jet velocity exceeds that of sound, i.e., for  $Ma > 1$ , the jet flow no longer varies smoothly and rather displays shock wave structures shown in Fig. 7 for  $Q = 1800$  sccm with  $Ma_{\max} =$

1.046, where a small shock wave zone (with local pressure ~3450 Pa below the ambient value  $10^5$  Pa) appears right at the exit of the jet orifice. Interestingly, the 1D isentropic flow theory would suggest a local pressure of 3600 Pa below the ambient value.

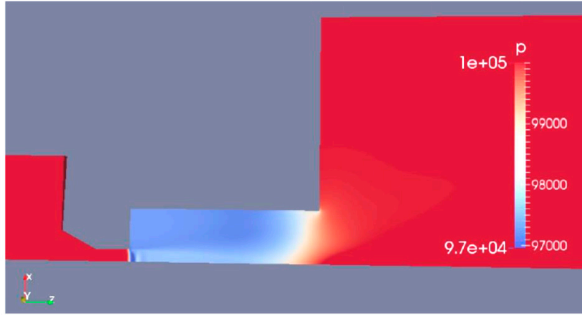


Fig. 7 The pressure field for  $Q = 1800$  sccm with  $Ma_{\max} = 1.046$

Despite the fact that the gas jet flow simulated here may differ considerably from that of simplified flow case, the 1D isentropic flow theory [9], i.e.,  $T_{\min} = 300 / (1 + 0.2 Ma^2)$  and  $\Delta P = [1 - (1 + P_g) / (1 + 0.2 Ma^2)^{3.5}] \times 10^5$ , can predict  $T_{\min}$  quite accurately and  $\Delta P$  reasonably well for  $Ma < 1$  based the computed values of  $Ma_{\max}$  and  $P_g$  given in Table I. For example, the value of  $\Delta P$  is calculated as 336, 891, 1508 and 2052 Pa for  $Q = 600, 900, 1200$  and  $1500$  sccm, respectively. When  $Ma_{\max} > 1$ , the value of  $\Delta P$  calculated from the 1D formula is only consistent with the lowest pressure value associated with the shock wave, not the negative pressure in most part of the jet expansion channel for liquid aspiration.

#### B. Variations with Jet Orifice of $D = 0.35$ mm

If the nominal case configuration is modified with the diameter of jet expansion channel reduced to  $D_e = 1.0$  mm (from the nominal 1.5 mm), the computed values of  $U_{\max}$ ,  $Ma_{\max}$ ,  $\Delta P$ ,  $P_g$ , and  $T_{\min}$  at various gas flow rates become those in Table II. Such a reduction of  $D_e$  tends to enhance  $\Delta P$  in the jet expansion channel by a factor of more than 3, with slightly increased jet velocity and  $Ma_{\max}$  at a given  $Q$ .

TABLE II  
AS TABLE I BUT FOR REDUCED EXPANSION CHANNEL DIAMETER

$Q$ (sccm)	$U_{\max}$ (m/s)	$Ma_{\max}$	$\Delta P$ (Pa)	$P_g$ (bar)	$T_{\min}$ (K)
600	138	0.403	1359	0.099	291
900	199	0.592	2904	0.221	280
1200	256	0.780	4946	0.401	267
1500	306	0.958	7377	0.639	253
1800	354	1.136	10052	1.017	241

In this case, the 1D isentropic flow theory would grossly overestimate the value of  $\Delta P$  based on the values of  $Ma_{\max}$  and  $P_g$  given in Table II. For example, the value of  $\Delta P$  would be calculated as 1732, 3675, 6266 and 9130 Pa for  $Q = 600, 900, 1200$  and  $1500$  sccm, respectively (for  $Ma_{\max} < 1$ ). Therefore, the 1D theory may be used for a rough sanity check of the CFD results, but should not be regarded as a reliable

predictive tool with acceptable accuracy.

Conversely, with increasing  $D_e$  to 1.7 mm (from 1.5 mm) the peak jet velocity for  $Q = 1200$  sccm is reduced from 246 to 244 m/s with  $Ma_{\max} = 0.741$ , and  $\Delta P$  becomes 828 Pa, much lower than 1524 Pa with the nominal configuration.

The effect of varying the jet expansion channel length  $L_e$  is examined by reducing  $L_e$  from 2.7 to 2.2 mm, with computed results shown in Table III. Shortening the jet expansion channel length tends to reduce the magnitude of negative pressure. Conversely, increasing  $L_e$  to 3.0 mm (with  $D_e = 1.5$  mm) could increase  $\Delta P$  to 1987 Pa (with  $Ma_{\max} = 0.749$ ,  $P_g = 0.423$  bar) for  $Q = 1200$  sccm.

TABLE III  
AS TABLE I BUT FOR REDUCED EXPANSION CHANNEL LENGTH

$Q$ (sccm)	$U_{\max}$ (m/s)	$Ma_{\max}$	$\Delta P$ (Pa)	$P_g$ (bar)	$T_{\min}$ (K)
600	136	0.397	195	0.113	291
900	193	0.573	461	0.244	281
1200	245	0.741	839	0.429	270
1500	289	0.896	1221	0.666	258
1800	326	1.034	1516	0.928	247

The reason for enhanced negative pressure by shrinking  $D_e$  and increasing  $L_e$  is simply that a narrower and longer channel corresponds to a greater pressure gradient for driving the same amount of back flow, to compensate the jet depleted gas in the jet expansion channel.

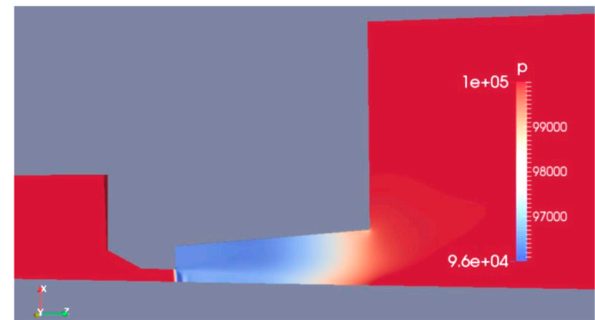


Fig. 8 The pressure field for  $Q = 1800$  sccm with  $Ma_{\max} = 1.054$  in a jet expansion channel with diameter increasing from 1.0 to 1.5 mm

If the jet expansion channel is arranged to have a diverging expansion channel (as shown in Fig. 8), Table IV indicates that the negative pressure therein is generally enhanced in comparison with the nominal configuration. The magnitude of negative pressure is somewhere in between of that of Table I and Table II, not surprisingly.

TABLE IV  
AS TABLE I BUT FOR A DIVERGING EXPANSION CHANNEL

$Q$ (sccm)	$U_{\max}$ (m/s)	$Ma_{\max}$	$\Delta P$ (Pa)	$P_g$ (bar)	$T_{\min}$ (K)
600	136	0.398	464	0.110	291
900	194	0.577	1058	0.239	281
1200	247	0.750	1929	0.423	270
1500	293	0.909	2667	0.659	257
1800	331	1.054	3309	0.926	245

Changing the jet expansion channel from diverging (as in Fig. 8) to converging, e.g., with diameter gradually decreasing from 1.5 to 1.0 mm with the axial distance  $z$ , the values of  $U_{\max}$ ,  $Ma_{\max}$ , and  $\Delta P$  for  $Q = 1200$  sccm become 253 m/s, 0.770, and 4863 Pa, respectively (approaching those corresponding values in Table II). Thus, the diameter of outlet of the jet expansion channel plays a more important role to influence the negative pressure magnitude, as expected from the fluid dynamics point of view.

It appears that the magnitude of negative pressure generally correlates with the value of  $Ma_{\max}$  of the jet flow. One of the effective ways to increase the Mach number at a given gas flow rate  $Q$  is to reduce the jet orifice size.

### C. Effects of Reducing Jet Orifice to $D = 0.25$ mm

By reducing the diameter of jet orifice  $D$  to 0.25 mm (from the nominal 0.35 mm), a given value of  $Ma_{\max}$  is expected to be obtained with a gas flow rate  $Q$  of about half that with the nominal  $D = 0.35$  mm, because the jet velocity is roughly given by  $4Q/(\pi D^2)$  and  $(0.25/0.35)^2 = 0.5102$ . Indeed the computed values of  $Ma_{\max}$  for  $D = 0.25$  mm at  $Q = 600$  sccm become 0.741 and 0.745 for the jet expansion channel with  $D_e = 1.5$  and 1.0 mm (at  $L_e = 2.7$  mm), respectively. This is quite comparable with  $Ma_{\max} = 0.746$  for the nominal case with  $D = 0.35$  mm (and  $D_e = 1.5$  mm with  $L_e = 2.7$  mm) in Table I.

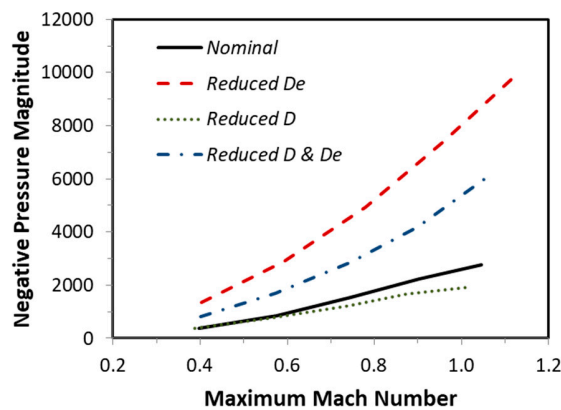


Fig. 9 Negative pressure magnitude  $\Delta P$  versus maximum Mach number  $Ma_{\max}$  for the nominal case, for  $D_e$  reduced from 1.5 to 1.0 mm, for  $D$  reduced from 0.35 to 0.25 mm (while  $D_e = 1.5$  mm), and for  $D_e = 1.0$  mm and  $D = 0.25$  mm

The general effects of varying  $D = 0.35$  to 0.25 mm and  $D_e = 1.5$  to 1.0 mm on  $\Delta P$  versus  $Ma_{\max}$  are shown in Fig. 9, with solid line for the nominal case ( $D = 0.35$  mm and  $D_e = 1.5$  mm with  $L_e = 2.7$  mm), dashed line for  $D_e$  reduced to 1.0 mm, dotted line for  $D$  reduced to 0.25 mm, and dash-dot line for  $D_e$  reduced to 1.0 mm while  $D = 0.25$  mm. It becomes clear that the most effective way to significantly increase  $\Delta P$  is to shrink the diameter of jet expansion channel  $D_e$ , e.g., from 1.5 to 1.0 mm. While reducing the jet orifice diameter  $D$  from 0.35 to 0.25 mm can increase  $Ma_{\max}$  by about a factor of two with a given gas flow rate  $Q$ , the value of  $\Delta P$  at a given  $Ma_{\max}$  is substantially reduced from that with  $D = 0.35$  mm for the

same jet expansion channel. Thus the ratio of  $D_e$  and  $D$  can be important, too. With  $D_e = 1.5$  mm,  $D_e/D = 4.286$  and 6.0 for  $D = 0.35$  and 0.25 mm, consistent with the expected effect of enhancing  $\Delta P$  by reducing  $D_e/D$  (as suggested by Table II).

Moreover, the length of jet expansion channel  $L_e$  also has a role to play for influencing the magnitude of negative pressure  $\Delta P$  (as shown with Table III). For a case of  $D = 0.25$ ,  $D_e = 1.0714$ , and  $L_e = 1.9286$  mm, the values of  $D_e/D$  and  $L_e/D$  are kept the same as that in Table I. The computed value of  $\Delta P$  then becomes 1412 Pa for  $Q = 600$  sccm with  $Ma_{\max} = 0.744$ , quite close to (or within 10% of) 1524 Pa for a similar value of  $Ma_{\max}$  in Table I. Despite the similarity of geometric configuration and the value of  $Ma_{\max}$ , reducing the jet orifice diameter leads to a considerable change of Reynolds number (i.e.,  $Re = 3513$  for  $D = 0.25$  mm at  $Q = 600$  sccm whereas  $Re = 5018$  for  $D = 0.35$  mm at  $Q = 1200$  sccm). Thus some difference in the value of  $\Delta P$  between  $D = 0.25$  and 0.35 mm (for the same  $Ma_{\max}$ ) should not be surprising.

## IV. DISCUSSION

From the presented CFD results, a general idea can be gained about the magnitude of negative pressure generated with the compressible gas jet flow in the jet expansion channel of a pneumatic atomizer (as variations of the Collison nebulizer). Whether the value of such a negative pressure  $\Delta P$  can account for the observed behavior of pneumatic atomization deserves an in-depth discussion.

According to the description of May [1] with measurements of a Collison nebulizer, the typical liquid aspiration rate is about  $Q_{\text{ink}} = 67$  ml/min (per jet) for water. This requires an extra pressure difference of about 180 Pa over the ink syphon tube with a length of  $L_s = 20$  mm and diameter of  $D_s = 1.5$  mm, assuming a liquid viscosity of  $\mu_{\text{ink}} = 1.0$  cp ( $= 0.001$  Pa s) in the Poiseuille equation for  $\Delta p = 128 \mu_{\text{ink}} L_s Q_{\text{ink}} / (\pi D_s^4)$ . Including the hydrostatic pressure (200 Pa for  $\rho_{\text{ink}} = 1.0$  g/cc), a total negative pressure of magnitude  $\Delta P = 380$  Pa (as might be obtained with a gas flow rate of  $Q = 600$  sccm) should be sufficient for syphoning water up at a rate of 67 ml/min.

However, the gas flow rate used with the Collison nebulizer was typically  $Q > 2000$  sccm [1], which is expected to produce much more negative pressure (e.g.,  $\Delta P > 3000$  Pa in view of Table I) than needed for just water aspiration. Hence, the syphoning rate of water is likely restricted by the amount of water accumulated in the jet expansion channel due to limited water removal rate by the blowing gas stream. There must be a dynamic balance between the liquid aspiration rate and the liquid removal rate in the jet expansion channel, for a sustainable continuous atomization. Data from rigorous measurements [4] indeed show an increase followed by a decrease in the liquid aspiration rate (in units of ml/min) with increasing air pressure  $P_g$  (or gas flow rate  $Q$ ) for several “air-jet” nebulizers, while all nebulizers tested show declining trends of liquid aspiration rate in units of “ml per liter of air” with increasing air flow rate (for  $Q > 2$  l/min).

On the other hand, most inks used in the Aerosol Jet® pneumatic atomizer usually have viscosity  $\mu_{\text{ink}} > 100$  cp (and

some may even reach 1000 cp), more than two orders of magnitude greater than that of water. For a comparable aspiration rate, syphoning the Aerosol Jet® inks would require a  $\Delta P > 18000$  Pa on top of the hydrostatic pressure (about 400 Pa), which does not seem possible with a gas flow rate  $Q < 2000$  sccm (in view of Table I). In realistic atomizer operation, however, the flow field in jet expansion channel is not a simplified single-phase gas flow as computed here; instead there is a rather complicated two-phase gas-liquid flow. If we take into account of the fact that part of the jet expansion channel would be filled with the syphoned liquid, the channel volume for gas-phase flow is reduced and the channel diameter effectively shrinks in a dynamic process of liquid being syphoned in and blown out. Reducing the diameter of jet expansion channel due to liquid holdup therein tends to enhance the negative pressure for syphoning (as shown in Table II, etc.), to produce an appropriate liquid aspiration rate. Thus, a dynamic balance of liquid holdup can be imagined as the more liquid syphoned into the channel the more liquid will be blown out for atomization. The exact amount of liquid holdup and shape of the gas-liquid free surface in the jet expansion channel require a technically challenging multiphase free-surface flow simulation with very fine discretization meshes, which is not further pursued in the present study.

At the minimum gas flow rate (e.g.,  $Q = 600$  sccm or so) for atomization, the magnitude of negative pressure  $\Delta P$  may only reach the threshold to bring liquid ink up to the jet expansion channel, with little extra for sustaining the expected liquid aspiration rate in the syphon tube. But as the liquid accumulates in the channel, the channel diameter shrinks and the magnitude of negative pressure increases, leading to greater liquid aspiration rate until a dynamic balance in the liquid holdup is established with the liquid removal rate.

The amount of liquid holdup in the jet expansion channel is expected to increase with the gas flow rate, up to a certain amount. Beyond an optimal value of the gas flow rate, at which the maximum output mist density is obtained, the liquid aspiration rate cannot increase proportionally to the gas flow rate; further increasing the gas flow rate effectively dilutes the mist even with more liquid being atomized. This could explain why the mist density output from the Collision nebulizer typically goes up and then down as the gas flow rate increases.

For Aerosol Jet® printing, the typical mist flow rate (through a single ink deposition nozzle) is less than 500 sccm, depending upon the nozzle size dictated by the desired print feature size. (To print fine feature about 10  $\mu\text{m}$  or less, the mist flow rate is usually less than 10 sccm with a deposition nozzle having a small outlet diameter of 100  $\mu\text{m}$ ). But the minimum gas flow rate for pneumatic atomizer to produce ink mist is usually more than 600 sccm (and typically around  $Q = 1200$  sccm for a maximized mist mass throughput with a given print feature size). Hence there is usually a substantial mismatch between the gas flow rate for ink atomization with the pneumatic atomizer and that of the mist flow for printing. Although such a mist flow rate mismatch problem may be solved by using a virtual impactor [2], reducing the gas flow

rate for adequate ink atomization remains as a desired attribute for the pneumatic atomizer improvement.

According to the present study, reducing the jet orifice diameter (e.g., from  $D = 0.35$  to 0.25 mm) can produce sufficient negative pressure in the jet expansion channel for ink aspiration at much reduced gas flow rate. But this modification may require a reduction of the diameter of jet expansion channel, too. Smaller channel is expected to reduce the liquid ink hold up therein for the gas stream to blow out and atomize. On the other hand, for a given  $Ma_{\text{max}}$  smaller jet orifice leads to a smaller amount of kinetic energy, which is often a key parameter for effective atomization [11] (because the physical process of atomization is in fact to convert part of the kinetic energy of gas jet flow into the surface energy of droplets). Therefore, the jet orifice diameter may not be reduced indefinitely for acceptable atomization performance; a minimum diameter is very likely to exist based on various practical considerations. More theoretical analysis and experimentation are required for optimizing the design of improved pneumatic atomizer for Aerosol Jet® printing as well as other applications.

## V. SUMMARY

The results of CFD simulations in the present work illustrate that the pressure distribution in the Collision nebulizer differs significantly from that of other fields with coherent characteristic structure, such as velocity, temperature, etc. A region of reduced pressure fills most of the jet expansion channel, creating a positive pressure gradient in the axial direction (i.e.,  $dp/dz > 0$ ) consistent with the sustained gas back flow surrounding the jet core in the jet expansion channel. Such a reduced pressure, or negative pressure of a magnitude  $\Delta P > 400$  Pa, could serve as the driving force for syphoning liquid ink from the ink reservoir into the jet expansion channel for subsequent atomization, enabling the Collision nebulizer to operate without requiring an active liquid pump.

The magnitude of negative pressure for a given gas flow rate appears to be quite sensitive to the geometric parameters of jet expansion channel. Among others, shrinking channel diameter can significantly enhance the negative pressure for liquid aspiration. This revealed behavior provides a logical explanation of the fact that the Collision nebulizer is quite capable of adequately atomizing liquids with a wide range of viscosity, even up to 1000 cp ( $= 1.0$  Pa s), using a gas flow rate  $Q < 2000$  sccm. Because adequate liquid aspiration plays a key role in effective ink atomization with Aerosol Jet® printing, the quantitative knowledge gained here with the CFD analysis is expected to help guide future development of more efficient pneumatic atomizers, with compressible flow of gas jet and associated negative pressure for liquid aspiration.

## ACKNOWLEDGMENT

The author would like to thank Dr. Andreas Mack of TNO Heat Transfer and Fluid Dynamics (Netherlands) for friendly sharing his knowledge in compressible turbulent flow



modeling, Mr. Dan Bachman and Mr. Dominick Carluccio of CH Technologies for carrying out intellectually inspiring experimental tests with various configurations of pneumatic nebulizers, and many Optomec colleagues for valuable technical discussions.

#### REFERENCES

- [1] K.R. May, "The Collision nebulizer: description, performance and application," *J. Aerosol Sci.*, vol. 4, pp. 235–243, May 1973.
- [2] <https://www.optomec.com/printed-electronics/aerosol-jet-technology/> (12/7/2017)
- [3] J.Q. Feng, "Multiphase flow analysis of mist transport behavior in Aerosol Jet® system," *Int. J. Comput. Meth. and Exp. Meas.*, vol. 6, no. 1, pp. 23–34, 2018.
- [4] R.W. Niven and J.D. Brain, "Some functional aspects of air-jet nebulizers," *Int. J. Pharmaceut.*, vol. 104, pp. 73–85, 1994.
- [5] D.R. Hess, "Nebulizers: Principles and performance," *Respiratory Care*, vol. 45, no. 6, pp. 609–622, June 2000.
- [6] <https://github.com/OpenFOAM/OpenFOAM-2.4.x> (12/7/2017)
- [7] P. O'Neill, J. Soria, and D. Honnery, "The stability of low Reynolds number round jets," *Exp. Fluids*, vol. 36 (3), pp. 473–483, 2004.
- [8] C. Gau, C.H. Shen, and Z.B. Wang, "Peculiar phenomenon of micro-free-jet flow," *Phys. Fluids*, vol. 21, 092001, 2009.
- [9] [https://web.stanford.edu/~cantwell/AA210A\\_Course\\_Material/](https://web.stanford.edu/~cantwell/AA210A_Course_Material/) (12/7/2017).
- [10] J.Q. Feng, "Sessile drop deformations under an impinging jet," *Theor. Comput. Fluid Dyn.*, vol. 29, issue 4, pp. 277–290, August 2015.
- [11] A. H. Lefebvre, *Atomization and Sprays*. New York: Hemisphere, 1989, ch. 1.